

Wiggly tails: a gravitational wave signature of massive fields around black holes

Juan Carlos Degollado^{1,2} and Carlos A. R. Herdeiro¹

¹ *Departamento de Física da Universidade de Aveiro and I3N,
Campus de Santiago, 3810-183 Aveiro, Portugal.*

² *Departamento de Ciencias Computacionales, Centro Universitario
de Ciencias Exactas e Ingeniería, Universidad de Guadalajara*

Av. Revolución 1500, Colonia Olímpica C.P. 44430, Guadalajara, Jalisco, México

(Dated: March 13, 2018)

Massive fields can exist in long-lived configurations around black holes. We examine how the gravitational wave signal of a perturbed black hole is affected by such ‘dirtiness’ within linear theory. As a concrete example, we consider the gravitational radiation emitted by the infall of a massive scalar field into a Schwarzschild black hole. Whereas part of the scalar field is absorbed/scattered by the black hole and triggers gravitational wave emission, another part lingers in long-lived quasi-bound states. Solving numerically the Teukolsky master equation for gravitational perturbations coupled to the massive Klein-Gordon equation, we find a characteristic gravitational wave signal, composed by a quasi-normal ringing followed by a late time tail. In contrast to ‘clean’ black holes, however, the late time tail contains small amplitude wiggles with the frequency of the dominating quasi-bound state. Additionally, an observer dependent beating pattern may also be seen. These features were already observed in fully non-linear studies; our analysis shows they are present at linear level, and, since it reduces to a 1+1 dimensional numerical problem, allows for cleaner numerical data. Moreover, we discuss the power law of the tail and that it only becomes universal sufficiently far away from the ‘dirty’ black hole. The *wiggly tails*, by contrast, are a generic feature that may be used as a smoking gun for the presence of massive fields around black holes, either as a linear cloud or as fully non-linear hair.

PACS numbers: 11.15.Bt, 04.30.-w, 95.30.Sf

I. INTRODUCTION

The forthcoming science runs of the second generation gravitational wave (GW) detectors [1], and, in parallel, the use of pulsar timing arrays [2], are promising a first direct detection of GWs from astrophysical sources before the decade is over. Such detection will initiate the field of *GW astrophysics*, a natural realm for testing general relativity in the strong field dynamical regime, as well as for constraining theoretical models that predict new gravitational interactions [3]. This new field should play a significant role over the next decades, delivering ever increasing precision measurements. Understanding such measurements requires theoretical guidance. As such, unveiling theoretical GW signatures of physical phenomena, and especially of new physics, is particularly timely.

Black holes (BHs) are the most compact objects predicted by general relativity. When involved in dynamical processes, they play a role as GWs sources. The GW emission pattern from a ‘clean’ (i.e. vacuum) perturbed BH has long been identified. The BH relaxes back to equilibrium via damped oscillations in characteristic frequencies – *quasi-normal ringing* [4] –, determined only by the final equilibrium state. A GW detector far from the BH will not only measure this ringing but also a late time tail [5], due to multiple scatterings by the space-time curvature of the GWs coming from the perturbed system. This late time tail has therefore the ability to probe the spacetime in the vicinity of the BH.

How does this simple picture change if the BH is ‘dirty’? That is, if it is surrounded by some matter/fields? In a recent thorough examination [6, 7], it was argued that the quasi-normal ringing will be unchanged, but that resonances could occur in the late time behaviour of waveforms. In this paper we shall present a clean resonance which is an effect in GW physics that may be used to identify a specific kind of ‘dirtiness’.

We consider a simple and tractable model of a dirty environment: a BH surrounded by a massive field. The field’s mass allows the existence of gravitationally trapped, long-lived field configurations around the BH, dubbed *quasi-bound states*, characterized by precise complex frequencies. Actually, massive field configurations can even become infinitely long-lived in the case of Kerr BHs, for a specific frequency determined by the horizon’s angular velocity [8–12]. The dynamical interaction of massive fields with BHs has been mostly discussed in the literature for scalar fields, both in the test field approximation (e.g. [13–15]) and in the fully non-linear regime [16, 17]. Our study also takes a scalar field as an illustrative case, but similar statements will hold for other massive fields, *e.g.*, Proca fields.

We show that the GW late time tail that follows the quasi-normal ringing of the BH, contains small amplitude oscillations with the (real part of the) frequency of the dominating quasi-bound state that endows the BH with a ‘dirty’ environment. These oscillations, which were first observed in [16] solving the non-linear Einstein-Klein-

Gordon system, are an imprint left by the field's cloud on the scatterings that originate the tail. Our setup, based on linear perturbation theory, confirms the generic behaviour described in [16], and clarifies it is essentially controlled by linear perturbations. Furthermore, the use of 1+1 evolutions allows us to optimize computational resources to extract physical signals.

The existence of these *wiggly tails* relies on two ingredients: a perturbed BH that relaxes by emitting GWs; and a dirty environment around the BH provided by a long lived configuration of a massive field, with one dominating oscillation frequency. This suggests that these tails may be considered as a strong evidence for the existence of massive fields around BHs.

We also discuss the power law decay of both the GW and scalar field tails. These have known universal exponents for clean BHs [18]. For the scalar case we find a generic decay as $R^{(s)} \sim t^{-2.5}$ as long as there are no quasi-bound state with significant amplitude at the extraction point. This is in agreement with the results in Ref. [13]. Otherwise, the scalar field decay is not a universal power-law any longer. For the GW tail, we find that, as long as the extraction point is sufficiently far away from the 'dirty' BH, it decays as $R^{(g)} \sim t^{-1.5}$. This is a different behaviour from 'clean' BHs, for which the Price decay law is $t^{-(2\ell+3)}$ with $\ell = 2$ [5]. Otherwise, the GW decay is affected by the dirtiness and no generic behaviour could be unveiled.

This paper is organized as follows: after this introduction we describe the scalar field in the background of a BH in section II. In section III we introduce the linear gravitational perturbation equations in terms of the Weyl scalar Ψ_4 as well as the harmonic decomposition to get a set of 1+1 coupled partial differential equations. In section IV we describe the numerical code used to solve them and the numerical results. Finally, in section V we give some concluding remarks.

II. A MODEL FOR A 'DIRTY' PERTURBED BLACK HOLE

As a simple model of a perturbed BH in a 'dirty' environment we shall consider the interaction of a Schwarzschild BH with a scalar field Φ , with mass μ and stress-energy tensor

$$T_{\mu\nu} = \Phi_{,\mu}\Phi_{,\nu} - \frac{1}{2}g_{\mu\nu}(\Phi^{,\sigma}\Phi_{,\sigma} + \mu^2\Phi^2) . \quad (1)$$

The conservation of the stress-energy tensor implies that the field obeys the Klein-Gordon equation $\square\Phi = \mu^2\Phi$. We write the background geometry in ingoing Kerr-Schild coordinates, which are horizon penetrating and hence more adequate for a numerical treatment. The corresponding line element is

$$ds^2 = -f(r)dt^2 + \frac{4M}{r}drdt + \left(1 + \frac{2M}{r}\right)dr^2 + r^2d\Omega_2 , \quad (2)$$

where $f(r) \equiv (1 - \frac{2M}{r})$ and $d\Omega_2$ is the standard line element on S^2 .

In order to find the solutions of interest of the Klein Gordon equation, the scalar field Φ can be expanded in Fourier modes of frequency ω and spherical harmonics $Y_0^{\ell,m}$ with spin weight zero. Requiring that the field is ingoing at the horizon and approaches zero at spatial infinity leads to a discrete set of complex frequencies, for each ℓ , corresponding to a fundamental mode and overtones. These solutions are the quasi-bound states. These states have well known frequencies of oscillation and rates of decay, *cf.* for instance [19–21], which depend on the value of μ . The trend to keep in mind, for the Schwarzschild background, is that increasing the mass of the scalar field implies decreasing the life-time of the quasi-bound states, which is measured by the (inverse of the) imaginary part of the complex frequencies. For very small μ , *e.g.* 10^{-23} eV, a value compatible with some scalar field dark matter models [22], quasi-bound states may last for cosmological time scales around a supermassive BH, say with $\sim 10^8 M_\odot$, without being significantly absorbed [14]. In such cases, the field configuration can be considered as a continuous source of perturbation. Below we shall give specific frequencies for the cases of interest herein, obtained using the continued fraction method first described in [23].

In this paper, we study the gravitational perturbations of the background sourced by the scalar field. These perturbations are evolved simultaneously with the Klein-Gordon equation in the unperturbed background, since the background perturbations lead to second order effects in the Klein-Gordon equation. The model is the following. We perturb the geometry by setting, at some initial time, a wave packet of the scalar field in the background (2). A generic wave packet contains a range of frequencies that includes quasi-bound state frequencies but also contains enough dynamics to awake the quasi-normal modes of the BH. Thus, in the evolution of the scalar field wave packet, there is a part which lingers around the BH in one dominating long-lived quasi-bound state. Other sub-leading quasi-bound states are also present, and lead to one observable effect, as we shall describe. Here, long-lived means that the time scale for the decay of the quasi-bound state is much longer than the time scale for the quasi-normal ringing.

III. SCALAR FIELD SOURCED GRAVITATIONAL PERTURBATIONS

To compute the GWs induced by the backreaction of the scalar field on the metric we use linear perturbation theory in the Newman-Penrose formalism. The radiative information is extracted from the Newman-Penrose scalar $\Psi_4 = -C_{\alpha\beta\gamma\delta}k^\alpha m^{*\beta} k^\gamma m^{*\delta}$, where $C_{\alpha\beta\gamma\delta}$ is the first order perturbed Weyl tensor, the vectors $(l^\alpha, m^\alpha, k^\alpha)$ are elements of a Newman-Penrose null basis [24, 25] and $m^{*\alpha}$ is the complex conjugate of m^α .

For distant observers, Ψ_4 describes outgoing GWs. A central observation, due to Teukolsky [26, 27], is that for (background) spacetimes of Petrov type D the first order perturbation of Ψ_4 decouples from the perturbations of the other Newman-Penrose scalars. Furthermore, he showed that the resulting wave equation can be separated in the Kerr (and thus Schwarzschild) background in its angular and radial parts, by expanding the perturbation in a basis of spheroidal harmonics with the appropriate spin weight.

To solve numerically the radial perturbation equation coupled to the Klein-Gordon equation we use the line element (2) and the null vector basis $k^\mu = (1, -1, 0, 0)$,

$$l^\mu = \frac{1}{2}(2 - f(r), f(r), 0, 0), \quad m^\mu = \frac{1}{\sqrt{2}r}(0, 0, 1, i \csc \theta).$$

The details of the derivation of the equation for the perturbed Weyl scalar Ψ_4 are given in [28]. After decomposing Ψ_4 in terms of spin weighted spherical harmonics (with weight -2):

$$\Psi_4 = \frac{1}{r} \sum_{\ell, m} R_{\ell, m}^{(g)}(t, r) Y_{-2}^{\ell, m}(\theta, \varphi), \quad (3)$$

the radial-temporal perturbation equation reads

$$\begin{aligned} & - \left(1 + \frac{2M}{r}\right) \partial_{tt} R_{\ell, m}^{(g)} + \left(1 - \frac{2M}{r}\right) \partial_{rr} R_{\ell, m}^{(g)} + \frac{4M}{r} \partial_{rt} R_{\ell, m}^{(g)} \\ & + 2 \left(\frac{2}{r} + \frac{M}{r^2}\right) \partial_t R_{\ell, m}^{(g)} + 2 \left(\frac{2}{r} - \frac{M}{r^2}\right) \partial_r R_{\ell, m}^{(g)} \\ & + \left(\frac{2M}{r^3} - \frac{(\ell-1)(\ell+2)}{r^2}\right) R_{\ell, m}^{(g)} = 16\pi r S(R_{\ell, m}^{(s)}), \end{aligned} \quad (4)$$

where the sources $S(R_{\ell, m}^{(s)})$, are projections of the stress-energy tensor (1) along the null tetrad; see for example Eqs. (3.10)-(3.21) of Ref. [28].

To solve the second order equation (4) we decompose it into a first order system using the first order variables

$$\psi_{\ell, m}^{(g)} \equiv \partial_r R_{\ell, m}^{(g)}, \quad \Pi_{\ell, m}^{(g)} \equiv \frac{r+2M}{r} \partial_t R_{\ell, m}^{(g)} - 2 \frac{M}{r} \psi_{\ell, m}^{(g)}. \quad (5)$$

Then, the following first order equations are obtained:

$$\partial_t R_{\ell, m}^{(g)} = \frac{1}{r+2M} \left(r \Pi_{\ell, m}^{(g)} + 2M \psi_{\ell, m}^{(g)} \right), \quad (6)$$

$$\partial_t \psi_{\ell, m}^{(g)} = \partial_r \left[\frac{1}{r+2M} \left(r \Pi_{\ell, m}^{(g)} + 2M \psi_{\ell, m}^{(g)} \right) \right], \quad (7)$$

$$\begin{aligned} \partial_t \Pi_{\ell, m}^{(g)} &= \frac{1}{r+2M} \left(2M \partial_r \Pi_{\ell, m}^{(g)} + r \partial_r \psi_{\ell, m}^{(g)} \right) \\ &+ \frac{2}{r(r+2M)^2} \left[(2r^2 + 5Mr + 4M^2) \Pi_{\ell, m}^{(g)} \right. \\ &+ (r+4M)(2r+3M) \psi_{\ell, m}^{(g)} \left. \right] \\ &+ \left(\frac{2M}{r^3} - \frac{(\ell-1)(\ell+2)}{r^2} \right) R_{\ell, m}^{(g)} - 16\pi r S(R_{\ell, m}^{(s)}) \end{aligned} \quad (8)$$

To compute the evolution of the source in (8), we must follow the dynamics of the scalar field, given by the Klein-

Gordon equation. We write this equation in the coordinates (2) and decompose the field as

$$\Phi = R_{\ell, m}^{(s)}(t, r) Y_0^{\ell, m}(\theta, \varphi). \quad (9)$$

Then a second order partial differential equation for $R_{\ell, m}^{(s)}(t, r)$ is obtained. In order to solve it, we perform a first order decomposition, in close analogy with that performed for the gravitational perturbations, by defining $\psi_{\ell, m}^{(s)} \equiv \partial_r R_{\ell, m}^{(s)}$ and

$$\Pi_{\ell, m}^{(s)} \equiv \frac{r+2M}{r} \partial_t R_{\ell, m}^{(s)} - 2 \frac{M}{r} \psi_{\ell, m}^{(s)}. \quad (10)$$

With these first order variables the Klein-Gordon equation becomes an evolution equation for $\Pi_{\ell, m}^{(s)}$,

$$\begin{aligned} \partial_t \Pi_{\ell, m}^{(s)} &= \frac{1}{r+2M} \left(2M \partial_r \Pi_{\ell, m}^{(s)} + r \partial_r \psi_{\ell, m}^{(s)} \right) \\ &+ \frac{2}{r(r+2M)^2} (\psi_{\ell, m}^{(s)} - \Pi_{\ell, m}^{(s)}) \\ &+ \left(\mu^2 - \frac{\ell(\ell+1)}{r^2} + \frac{2M}{r^3} \right) R_{\ell, m}^{(s)}. \end{aligned} \quad (11)$$

With the solution of the scalar field at each time step we reconstruct the stress-energy tensor of the scalar field (1) and then the source term in (8).

IV. NUMERICAL RESULTS

We numerically solved the coupled system (6)–(8) and (10)–(11), for the evolution of the gravitational perturbations and of the scalar field. We have used the method of lines with a third order Runge Kutta time integration and finite differencing with sixth order stencils. Such accuracy is needed in order to capture correctly the late time tail behaviour. The use of horizon penetrating coordinates allow us to set the inner boundary inside the horizon. The outer boundary is typically located at $r = 1000M$ (although in some cases we set it at $r = 2000M$ in order to avoid any contamination coming in from the boundary). At the last point of the numerical grid we set up the incoming modes to zero.

We chose as initial data a static Gaussian perturbation of the scalar field, with the form $R_{1,0}^{(s)}(0, r) = e^{-(r-r_g)^2/\sigma^2}$. For a typical run, the pulse was centred at $r_g = 10M$ and $\sigma = 0.5M$. The gravitational perturbation is initially set to zero, since we are interested in the gravitational waveform produced as a response to the presence of the scalar field. This choice of initial data does not bias the result. It has been observed, by numerically evolving arbitrary initial data, that the appearance of quasi-bound states is generic [29]. This guarantees that our choice of initial data will create the ‘dirty’ environment we seek and simultaneously excite the quasi-normal ringing of the BH; but other choices would also achieve the same goal. Indeed, we observe that part of

the scalar field falls into the BH, part is scattered and another part remains as quasi-bound states.

Fig. 1 exhibits the gravitational signal for $M\mu = 0.48$, as measured by a sufficiently distant observer. As expected, the quasi-normal ringing is followed by a late time tail. We have found that the dirtiness is negligible for the ringing, in agreement with the results in [6, 7]: performing a sinusoidal fit of the first stages of the signal, we obtained that the quasi-normal ringing has the frequency of the quadrupolar ($\ell = 2$) gravitational mode $\omega^{QNM} = 0.373 - i 0.0889$ of a clean Schwarzschild BH [4, 18, 30].

A careful inspection of the late time behaviour, on the other hand, unveils a novel feature: on top of the decaying behaviour there are oscillations with a very small amplitude – Fig. 1 (inset). The frequency of the oscillations in this *wiggly tail* precisely correspond to the real part of the frequency of the dominating, *i.e.* largest amplitude, quasi-bound state. In this case the dominating state is the first overtone, with frequency $\omega_1 = 0.4717 - i 1.4501 \times 10^{-3}$ [14].

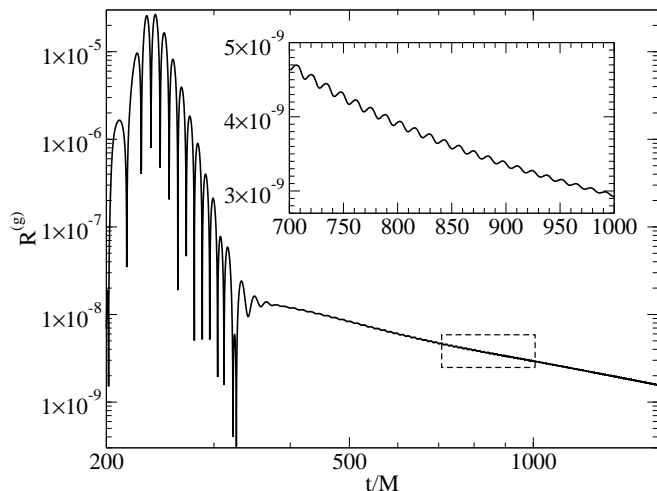


FIG. 1: GW signal ($\ell = 2$) for $M\mu = 0.48$ (observer at $500M$). Small amplitude wiggles can be seen in the late time behaviour, in an otherwise apparently power law tail.

To clearly demonstrate the observation in the last paragraph and simultaneously exhibit yet another effect that may be present in the late time signal, we present a slightly different value of the field’s mass $M\mu = 0.4$, for which we monitor the behaviour of both the scalar field and of the GW signal – Fig. 2. In this figure, the GW signal has been rescaled for better visualization. The first observation is that the late time GW signal (black solid line) presents, besides the aforementioned wiggles, a *beating* pattern. The figure shows that the beating in the GW signal is resonating the beating observed in the scalar field. Beating patterns are typical in systems with two dominating frequencies with comparable amplitudes. In this case, the beating frequency corresponds to the difference between the first and second overtones.

The second observation is that the frequency of the wiggles seen in the late time GW signal coincides with the frequency of the dominating quasi-bound state(s). This is shown in the figure’s inset.

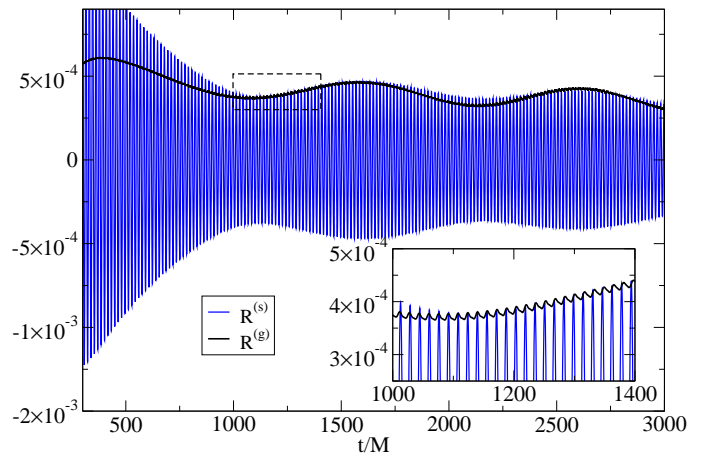


FIG. 2: Scalar ($\ell = 1$) and GW ($\ell = 2$) signal for $M\mu = 0.40$ (observer at $70M$). The dominant frequency of the scalar field is that of the first quasi-bound state overtone, with $\omega_1 = 0.3955 - i 2.2668 \times 10^{-4}$; the next leading quasi-bound state is the second overtone, with $\omega_2 = 0.3975 - i 1.0035 \times 10^{-4}$.

Both the reported effects seen in the late time tails – the wiggles and the beating – depend on the value of the field’s mass μ . For the wiggles, the mass yielding the largest amplitude is $M\mu \simeq 0.48$. One may think of this optimal mass as a balance between two effects. Smaller μ increases the life-time of the ‘dirtiness’; however, it also increases its spatial dispersion, and thus decreases the local effect of the perturbation. For the beating, the dominating quasi-bound states should have comparable amplitudes and the difference in frequencies should yield a period compatible with the observation times. An empirical conclusion, for our sets of initial data, is that the beating is most visible for $M\mu \simeq 0.4$ – Fig. 3.

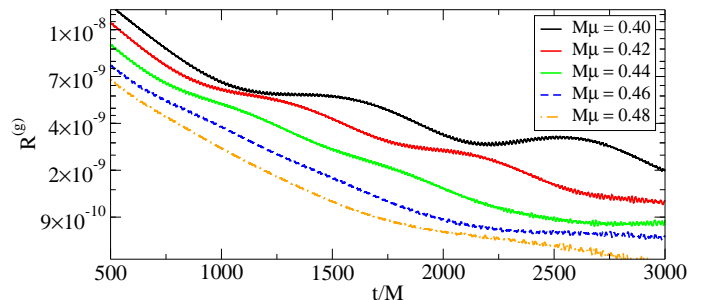


FIG. 3: Late time behaviour of the GW signal ($\ell = 2$) for several values of $M\mu$ (observer at $70M$). The beating becomes increasingly more visible as the mass is decreased from $M\mu = 0.48$ to $M\mu = 0.4$. For even smaller values the beating becomes again suppressed (not shown).

The existence of beating patterns for scalar fields around BHs has been discussed previously in different models [15, 16, 31]. But the study herein first reports a GW signal clearly resonating with such beating. We notice, however, that the beating – unlike the wiggles – depends on the extraction radius. For instance, if the observation point is close to any of the nodes of one of the states contributing to the beating, this effect vanishes both in the scalar field and in the GW counterpart. Furthermore, the beating is sensitive to the initial data, since, although quasi-bound states are excited for generic initial data, the amplitudes of these states depend on the details of such data.

Finally, we have observed that the late time behaviour of the GW signal has a power law when extracted sufficiently far away from the ‘dirty’ BH - Fig. 4. If the extraction takes place within the ‘dirtiness’, this is not the case, as illustrated by the curve with $M\mu = 0.1$ in Fig. 4, since for this value of the mass, the dominant quasi-bound state has a significant amplitude at the extraction position.

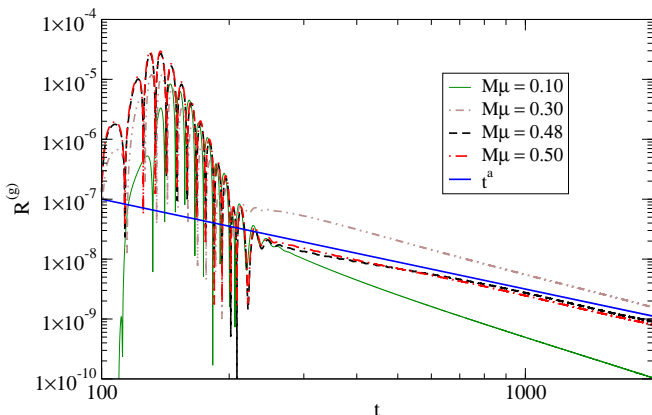


FIG. 4: Quadrupolar GW signal (observer at $100M$). We show a power law fit t^a with $a = 1.5$ for the late time tail. This power law fits well the three curves with highest mass, but it fails for the lowest mass.

V. CONCLUDING REMARKS

We have shown that the presence of a massive field in long-lived configurations around a BH leaves a distinctive signature in the late time behaviour of the GW signal when the BH is perturbed: a wiggly tail. The frequency of these wiggles is determined by the mass of the BH. For stellar mass BHs, $M \sim 1M_\odot - 10M_\odot$, this frequency lies in the range $\omega \sim 12.7 \text{ kHz} - 1.27 \text{ Hz}$, which, as for the corresponding quasi-normal modes, falls in the bandwidth of ground base detectors such as aLIGO [32]. For supermassive BHs, on the other hand, $M \sim 10^6M_\odot - 10^9M_\odot$, $\omega \sim 12.7 \text{ mHz} - 12.7\mu\text{Hz}$, entering the bandwidth of the space based detectors such as eLISA [3]. The amplitude

of the wiggles, however, is 10^4 times smaller than that of the corresponding quasi-normal modes. As such the detection of such a signal will be a considerable technical challenge.

Concerning the mass of the scalar field, the values considered here $M\mu \sim 0.4 - 0.5$, correspond to $\mu \sim 10^{-17} - 10^{-20} \text{ eV}$, for supermassive BHs and $\mu \sim 10^{-11} - 10^{-12} \text{ eV}$ for stellar mass BHs. Whereas these values are extremely small when compared to the masses of standard model particles, such light particles have been suggested in the context of high energy physics scenarios beyond the standard model. For instance, they arise naturally in string compactifications, *i.e.* the axiverse [33].

Both the existence of wiggles and of a beating in the GW tails are qualitative features that may be used to distinguish a dirty environment from an isolated BH. Interestingly, the mere presence of a beating is significant, since it provides evidence for two comparable amplitude frequencies in the dirty environment. For instance, for a Kerr BH with scalar hair [9], there should be a clearly dominating frequency – that of the background scalar field – and hence no noticeable beating should occur.

The observation of any of these features provides a quantitative measure of the frequencies of the quasi-bound states involved in the ‘dirtiness’ and hence of the mass of the field surrounding the BH.

Acknowledgements

We would like to thank Vitor Cardoso for useful comments on a draft of this paper. This work was partially supported by the NRHEP295189 FP7-PEOPLE-2011-IRSES Grant. J.C.D. acknowledges support from FCT via project No. PTDC/FIS/116625/2010.

-
- [1] S. Hild, *Class.Quant.Grav.* **29**, 124006 (2012), 1111.6277.
- [2] G. Hobbs, A. Archibald, Z. Arzoumanian, D. Backer, M. Bailes, et al., *Class.Quant.Grav.* **27**, 084013 (2010), 0911.5206.
- [3] P. A. Seoane et al. (eLISA Collaboration) (2013), 1305.5720.
- [4] E. Berti, V. Cardoso, and A. O. Starinets, *Class.Quant.Grav.* **26**, 163001 (2009), 0905.2975.
- [5] R. H. Price, *Phys. Rev.* **D5**, 2419 (1972).
- [6] E. Barausse, V. Cardoso, and P. Pani (2014), 1404.7140.
- [7] E. Barausse, V. Cardoso, and P. Pani (2014), 1404.7149.
- [8] S. Hod, *Phys.Rev.* **D86**, 104026 (2012), 1211.3202.
- [9] C. A. R. Herdeiro and E. Radu, *Phys.Rev.Lett.* **112**, 221101 (2014), 1403.2757.
- [10] S. Hod, *Eur.Phys.J.* **C73**, 2378 (2013), 1311.5298.
- [11] C. Herdeiro and E. Radu, *Phys.Rev.* **D89**, 124018 (2014), 1406.1225.
- [12] C. A. R. Herdeiro and E. Radu (2014), 1405.3696.
- [13] L. M. Burko and G. Khanna, *Phys.Rev.* **D70**, 044018 (2004), gr-qc/0403018.
- [14] J. Barranco, A. Bernal, J. C. Degollado, A. Diez-Tejedor, M. Megevand, et al., *Phys.Rev.* **D84**, 083008 (2011), 1108.0931.
- [15] H. Witek, V. Cardoso, A. Ishibashi, and U. Sperhake, *Phys.Rev.* **D87**, 043513 (2013), 1212.0551.
- [16] H. Okawa, H. Witek, and V. Cardoso, *Phys.Rev.* **D89**, 104032 (2014), 1401.1548.
- [17] F. Guzman and F. Lora-Clavijo, *Phys.Rev.* **D85**, 024036 (2012), 1201.3598.
- [18] K. D. Kokkotas and B. G. Schmidt, *Living Reviews in Relativity* **2** (1999).
- [19] S. L. Detweiler, *Phys.Rev.* **D22**, 2323 (1980).
- [20] T. Zouros and D. Eardley, *Annals Phys.* **118**, 139 (1979).
- [21] S. R. Dolan, *Phys.Rev.* **D76**, 084001 (2007), 0705.2880.
- [22] T. Matos and L. A. Urena-Lopez, *Phys.Rev.* **D63**, 063506 (2001), astro-ph/0006024.
- [23] E. Leaver, *Proc.Roy.Soc.Lond.* **A402**, 285 (1985).
- [24] E. T. Newman and R. Penrose, *J. Math. Phys.* **3**, 566 (1962), erratum in *J. Math. Phys.* **4**, 998 (1963).
- [25] S. Chandrasekhar, *The Mathematical Theory of Black Holes* (Oxford University Press, Oxford, England, 1983).
- [26] S. Teukolsky, *Phys.Rev.Lett.* **29**, 1114 (1972).
- [27] S. A. Teukolsky, *Astrophys.J.* **185**, 635 (1973).
- [28] D. Nunez, J. C. Degollado, and C. Moreno, *Phys.Rev.* **D84**, 024043 (2011), 1107.4316.
- [29] J. Barranco, A. Bernal, J. C. Degollado, A. Diez-Tejedor, M. Megevand, et al., *Phys.Rev.Lett.* **109**, 081102 (2012), 1207.2153.
- [30] R. Konoplya and A. Zhidenko, *Rev.Mod.Phys.* **83**, 793 (2011), 1102.4014.
- [31] J. C. Degollado and C. A. R. Herdeiro, *Phys.Rev.* **D89**, 063005 (2014), 1312.4579.
- [32] G. M. Harry (LIGO Scientific Collaboration), *Class.Quant.Grav.* **27**, 084006 (2010).
- [33] A. Arvanitaki, S. Dimopoulos, S. Dubovsky, N. Kaloper, and J. March-Russell, *Phys.Rev.* **D81**, 123530 (2010), 0905.4720.